

Covalent immobilization of antibodies on electrochemically functionalized carbon surfaces

Stéphanie Dauphas,^a Anne Corlu,^b Christiane Guguen-Guillouzo,^b
Soraya Ababou-Girard,^c Olivier Lavastre^a and Florence Geneste^{*a}

Received (in Montpellier, France) 31st January 2008, Accepted 5th February 2008

First published as an Advance Article on the web 5th March 2008

DOI: 10.1039/b801743c

A general method is described for the covalent attachment to carbon surfaces of sensitive biomolecules such as antibodies. First, *N*-hydroxysuccinimide-activated carbon surfaces are prepared by a step by step method involving an electrografting process and a monoprotected homobifunctional linker to ensure a good control of the surface modification. Then, antibodies are introduced, at the last step of the modification procedure, under native conditions at physiological pH, to minimize their denaturation. Comparison with a classical method involving a homobifunctional linker shows a decrease of the degree of coverage of the surface by antibodies, explained by the formation of bridged structures by the linker.

Introduction

Carbon materials are extensively used as supports for biosensing applications, due to their interesting electrochemical properties as their wide potential window, the large variety of available carbon materials (*e.g.*, nanotubes, fibers, screen-printed electrodes, *etc.*) and the possibility to achieve stable covalent linkage on their surface. One method for the covalent immobilization of biomolecules on carbon consists in the creation of functional groups such as carboxylic, carbonyl, lactone and hydroxyl groups on its surface by chemical or electrochemical oxidations.^{1–3} The biomolecules are then anchored through a linker to the reactive surface. However, the oxidative treatments to generate the reactive surface also led to a partial degradation of carbon with the formation of blisters on its surface, affecting the sensor response.^{4,5}

Modification of carbon surfaces can also be achieved using less drastic electro-assisted methods.^{6–8} One of the most used process is the reduction of diazonium salts, providing aryl radicals, which react with the surface to give carbon–carbon covalent bond.⁹

The immobilization of biomolecules on carbon, based on this electrochemical procedure, has been reported.^{10–18} A first approach deals with the chemical modification of biomolecules to introduce aryl diazonium functions, allowing their electrochemical immobilization.^{10–12} However, the strong acidic conditions employed for the diazotation step can be incompatible with biomolecules, which are sensitive to their physiological environments, and can denature them.

Other strategies consist in the covalent binding of linkers on carbon surface and subsequent anchoring of biomolecules.^{13–19}

Thus, Hamers and co-workers^{14,15} have modified different carbon surfaces with a functionalization procedure involving 4-nitrobenzenediazonium salts²⁰ to achieve electrically addressable biomolecular functionalization. The subsequent cathodic reduction of the nitro groups afforded available aniline functions on specific nanostructures, thereby allowing the anchoring of DNA *via* an appropriate linker only on these nanostructures. Another method using 4-carboxybenzenediazonium salts has also been reported for direct immobilization of DNA on gold surfaces.¹⁹ This method presents the advantage of being simple because it does not involve the use of a linker, but can lead to the denaturation of the protein resulting in the loss of their functions, for example when employed with enzymes or antibodies. It is well known that the use of a long and flexible spacer provides greater accessibility of the antibody and minimizes its denaturation, reducing the steric interference with the surface and between antibodies.^{21,22}

Herein, we propose to extend the functionalization procedure involving 4-nitrobenzenediazonium salts to proteins such as antibodies, offering a general method for the covalent immobilization of this large protein family on carbon surfaces. As lysine is one of the most abundant amino-acids in proteins, we focused our attention on linkers reacting both with amino groups of lysine and aniline functions introduced onto the carbon surface. The method used a monoprotected homobifunctional linker to ensure a good control of the surface modification. The coverage of the surface was compared to a classical method involving a homobifunctional linker. Advantageously, the linker belongs to a family of commercially available compounds with different lengths of carbon chain and gives rise to a grafting process involving simple and quantitative chemical reactions such as acylation reaction, saponification and conventional *N*-hydroxysuccinimide (NHS)/1-(3-dimethyl-aminopropyl)-3-ethylcarbodiimide hydrochloride (EDC) chemistry. Biomolecules are then introduced in the last step of the grafting process under native conditions at physiological pH to minimize their denaturation.

^a Université de Rennes 1, UMR-CNRS 6226, Laboratoire des Sciences Chimiques de Rennes, Equipe catalyse et organométalliques, Campus de Beaulieu, 35042 Rennes cedex, France

^b Université de Rennes 1, INSERM U522, IFR 140, Campus de Villejean, 35042 Rennes cedex, France

^c Université de Rennes 1, UMR 6627, Laboratoire de Physique des Atomes, Lasers, Molécules et Surfaces, Campus de Beaulieu, 35042 Rennes cedex, France

Results and discussion

A polished graphite surface **1** was derivatized by the electrochemical reduction of 4-nitrobenzenediazonium salts (Scheme 1).

The nitro groups did not only serve as precursors to amino groups, but also as redox probes, allowing the estimation of surface concentration Γ of grafted aryl groups.⁵ The value of Γ ($9 \pm 2 \times 10^{-9}$ mol cm⁻² of geometric area), calculated from cyclic voltammetry analysis of the NHOH/NO reversible system (Fig. 1), was higher than a close-packed monolayer of 4-substituted phenyl groups (1.35×10^{-9} mol cm⁻²)⁷ estimated from molecular models.

This difference can be explained by the roughness of the polished graphite surface and by the formation of multilayers with protruding features on the surface, as previously observed with derivatization of carbon surfaces by cathodic reduction of diazonium salts.⁷ The nitro group of **2** was then electrochemically reduced in amine **3** at -1 V_{SCE} until the NHOH/NO reversible system disappeared. The amine **3** was then allowed to react with 5-chlorocarboxyl-pentanoic acid methyl ester to give **4** (Scheme 1; route 1). We have chosen this monoprotected homobifunctional linker to improve loading capacities of the modified surface, avoiding the formation of bridged structures with both ends fixed to the surface.²³ After

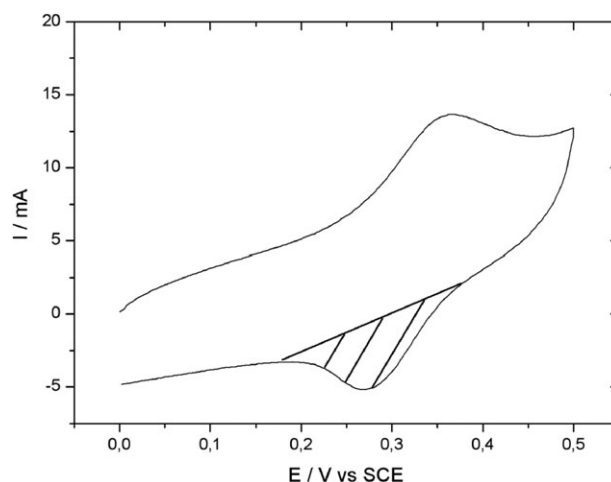
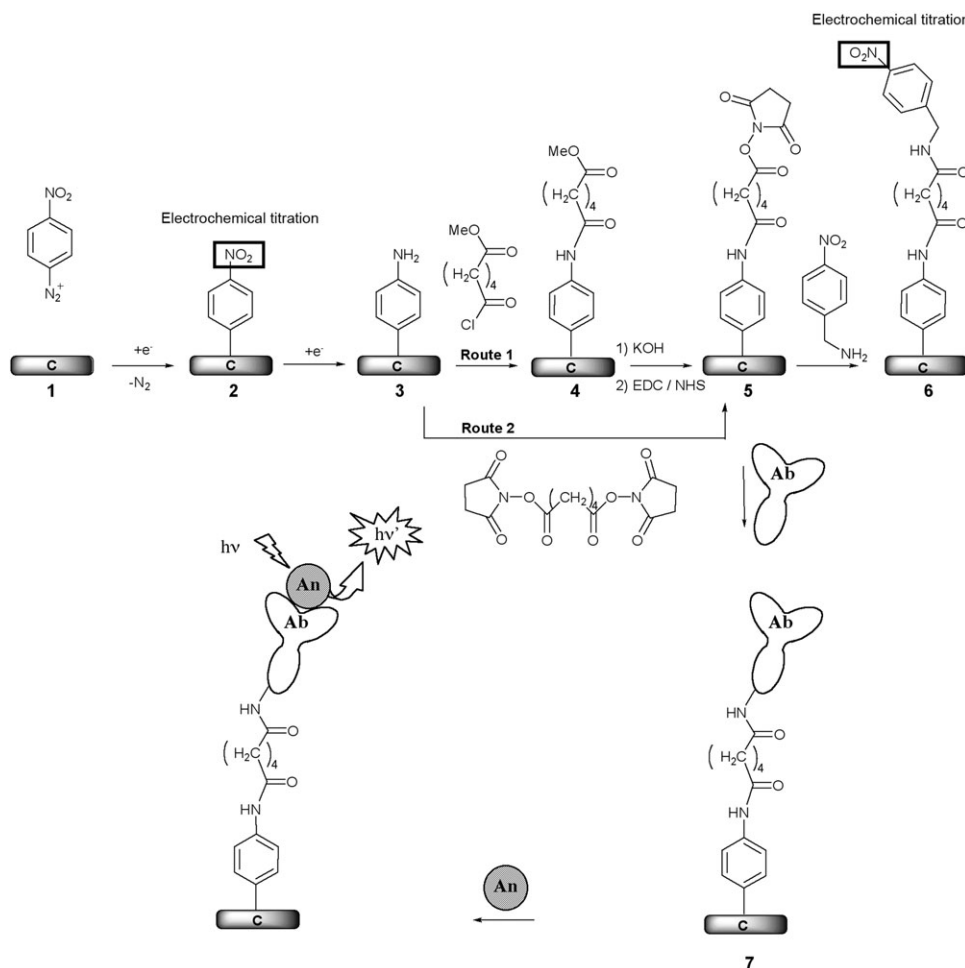


Fig. 1 Typical voltammogram of NHOH/NO system obtained in 0.5 M H₂SO₄ for nitro species present on the graphite surface, after reduction of NO₂ into NHOH at -0.5 V_{SCE}. Scan rate: 0.1 V s⁻¹. Only the bottom of the wave (*e.g.* hatched area) was considered for calculation of the surface concentration using the Faraday law.

deprotection by saponification, the resulting carboxylic acid was activated by reaction with 1-(3-dimethyl-amino-propyl)-3-ethylcarbodiimide hydrochloride (EDC) and



Scheme 1 Step by step method for the immobilization of antibodies and antigen-antibody recognition.

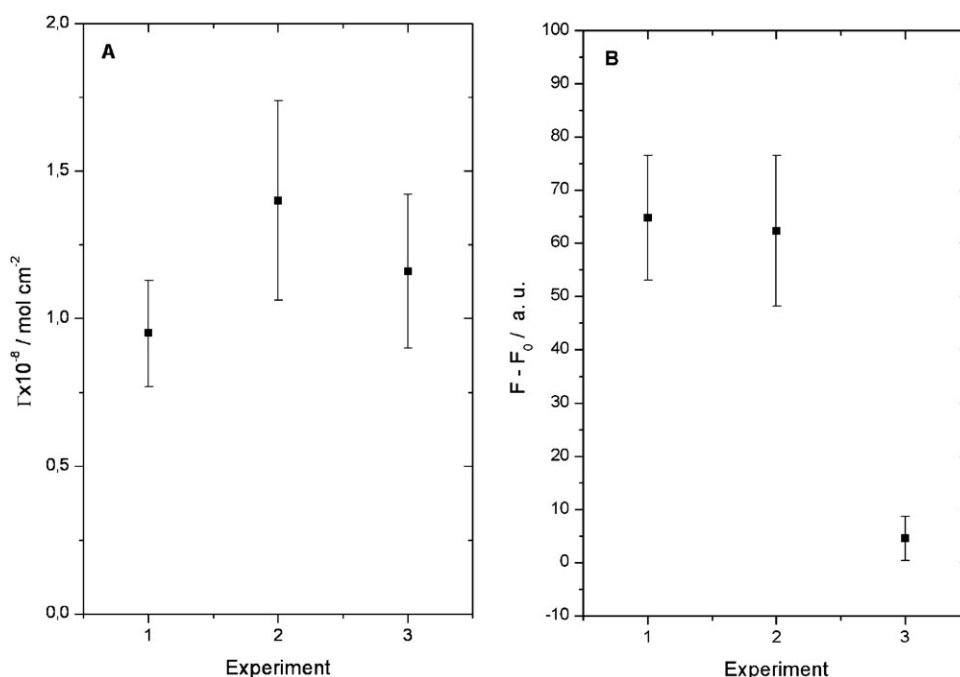


Fig. 2 Reproducibility measurements: (A) Surface concentrations Γ estimated by cyclic voltammetry of the nitrophenyl derivatized surfaces **2** (1) and of the NO_2 -linker-surfaces **6** prepared according to routes 1 (2) and 2 (3). (B) Fluorescent analysis of the antibodies modified surfaces **7** in the presence of fluorescent transferrin antigens, alone (1) or in competition with human albumin (2) and non-labelled antigens (3). F is the fluorescence intensity obtained in the presence of fluorescent transferrin antigens and F_0 is the signal in absence of antigen.

N-hydroxysuccinimide (NHS) to give **5**. At this stage, reaction with 4-nitrobenzyl amine was performed to check that all the modification process of the graphite surface had really been achieved and that the modified surface was reactive with amines at physiological pH (PBS: pH 7.4 phosphate buffered saline). Surface concentration Γ of $1.4 \pm 0.4 \times 10^{-8} \text{ mol cm}^{-2}$ was estimated from the electrochemical analysis of the nitro group of **6**. The value is close to that obtained for derivatization by 4-nitrobenzenediazonium salts, showing the efficiency of the immobilization process. The difference between the two values cannot be explained by adsorption of 4-nitrobenzylamine hydrochloride at the surface of the electrode since meticulous washing procedures were used (ultrasonication for 4.5 h in 6 different solvents). A study on nitrophenyl films grafted by electroreduction of 4-nitrobenzenediazonium salts has recently shown that some of the immobilized nitro groups were no more electroactive.²⁴ This phenomenon can explain the difference obtained between the two surface concentrations estimated by electrochemical analyses of the nitro groups.

For comparison, the amine **3** was allowed to react with hexanedioic acid bis-(2,5-dioxo-pyrrolidin-1-yl) ester (Scheme 1; route 2) and then with 4-nitrobenzyl amine.

A surface concentration of $1.0 \pm 0.26 \times 10^{-8} \text{ mol cm}^{-2}$ was estimated. If we consider a complete coverage of the surface, the difference with the surface concentration obtained with the monoprotected linker, can be interpreted by the formation of bridged molecular structures by the linker on the surface. The results of reproducibility measurements based on at least 5 experiments are given in Fig. 2A.

These electrochemical analyses were corroborated by XPS (X-ray photoelectron spectroscopy) analyses. The attachment of the linker to the surface **5** was confirmed by the increase of the N/C ratio compared with the reference electrode **1**, due to the presence of amide and succinimide groups (Table 1).

Anti-human transferrin antibodies were then covalently immobilized by reaction with the *N*-hydroxysuccinimide-activated carbon surfaces **5**. After rinsing with a solution of PBS, the samples were analyzed by XPS (Table 1). A large increase of the $\text{N}_{1s}/\text{C}_{1s}$ percent associated with the appearance of a peak of $\text{S}_{2p1/2+3/2}$ showed the presence of anti-transferrin antibodies on the graphite surface **7**. For comparison, the amine **3** was allowed to react with hexanedioic acid bis-(2,5-dioxo-pyrrolidin-1-yl) ester (Scheme 1; route 2) and then with anti-human transferrin antibodies under the same conditions. The $\text{N}_{1s}/\text{C}_{1s}$ content also increased, owing to the presence of

Table 1 Nitrogen and sulfur values as deduced from XPS analyses of modified graphite surfaces

| Nitrogen and sulfur/ carbon ratio | Fresh graphite 1 | <i>N</i> -Hydroxysuccinimide modified graphite 5 | Anti-transferrin antibodies modified graphite 7 | |
|--------------------------------------|-------------------------|--|--|-------------|
| | | | Via route 1 | Via route 2 |
| % N_{1s} 400–401 eV | 2–3 | 4–6 | 13 | 15 |
| % $\text{S}_{2p1/2+3/2}$ 164 eV | 0 | 0 | 0.5 | 0.2 |

CON groups in proteins and in the linker (Table 1). Interestingly, the $S_{2p1/2+3/2}/C_{1s}$ percent (0.2%) was significantly lower than the value previously obtained using the route 1 (0.5%). The $S_{2p1/2+3/2}$ peaks observed after anchoring of the anti-human transferrin antibodies according to routes 1 and 2 are given in Fig. 3.

Since antibodies are the only source of sulfur, the difference between the two peaks revealed a better degree of coverage of the surface modified according to route 1. This result was in accordance with cyclic voltammetry analyses (see above) and showed that the formation of bridged structures had an influence on the surface coverage of antibodies.

The effectiveness of the grafting process was also examined by AFM (atomic force microscopy). Fig. 4 shows the contact mode AFM images obtained in PBS of $5\ \mu\text{m} \times 5\ \mu\text{m}$ area of polished carbon **1**, *N*-hydroxysuccinimide-activated surfaces **5** and surfaces with covalently anchored antibodies **7**.

Average line profiles along a $5\ \mu\text{m}$ line are also given to estimate the variation in *z*-axis height. As seen in Fig. 4a, the roughness obtained for the polished carbon surface is in the range of previously reported values for this type of surface ($44\ \text{nm} \pm 6\ \text{nm}$).²⁵ After derivatization and introduction of the linker, surfaces changed their morphology with an apparent smoothing of the surface (Fig. 4b). This phenomenon is more visible on the deflection images, perhaps more sensitive to the surface relief pattern. Further introduction of anti-transferrin antibodies led to a complete coverage of the graphite surface, as seen in Fig. 4c. The image contained globular structures scattered uniformly on the surface. The diameter of the globules ranges from 50 to 500 nm. These structures can be attributed to aggregated antibody units attached to the surface. The difference in morphology observed for each step of the functionalization procedure confirmed the success of the grafting process. We also wanted to check that the dense layer imaged by AFM was not only due to adsorption of proteins on the organic layer **5** but to covalent immobilization. Among the different methods commonly used to desorb proteins from surfaces, we probably choose the most drastic one, ultrasoni-

cation in PBS, avoiding by this way the use of detergent, which can be a source of pollution for AFM analyses. The obtained topography (Fig. 4d) was similar to the previous one (Fig. 4c). Some differences in the peaks shape in the average line profiles were observed and can be explained by a partial degradation of the 3D-structure of the proteins during the ultrasonic treatment. Moreover, adsorption of anti-transferrin antibodies directly on graphite (with non-covalent coating of the surface) led, after ultrasonication in PBS, to images corresponding to a fresh polished graphite surface (data not shown). These results indicate that the covalent grafting process allows the formation of a stable and compact layer of proteins on the carbon surface.

Since AFM analyses did not allow us to discriminate between the fixation of antibody and antigen, we used a fluorescence microscopy approach to confirm anti-transferrin antibodies attachment and functionality following our protocol of immobilization. The aim was not to find the minimum of sensitivity, but to show that antibodies, immobilized according to our grafting procedure, specifically recognized antigens. Graphite surfaces coated with anti-transferrin antibodies were first saturated by a solution of delipidated fraction V bovine serum albumin (BSA) to avoid non-specific binding of antigens. Then, apo-transferrin labelled with Texas Red as fluorescent dye in BSA solution was incubated with the coated surface. Fixation of the antigen induced an increase of the fluorescent intensity quantitated as mean grey per pixels (Fig. 2B). To assess the specificity of the antibody–antigen reaction, we performed antigen competition experiments. When, the Texas Red labelled-apo-transferrin was incubated with the surface in presence of a 100 fold higher concentration of human serum albumin, no decrease in the fluorescence intensity was evidenced (Fig. 2B). In contrast, when the incubation of Texas Red labelled apo-transferrin was performed with a 100 fold higher concentration of non-labelled apo-transferrin, a drastic decrease in fluorescence intensity was detected. These experiments showed that specific antigen–antibody recognition is maintained when antibodies are anchored following our immobilization protocol. Reproducibility based on 8 different fluorescent measurements is given in Fig. 2B.

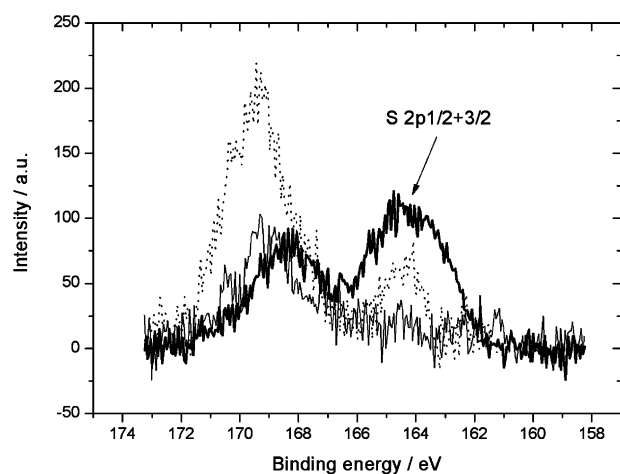


Fig. 3 $S_{2p1/2+3/2}$ spectra of *N*-hydroxysuccinimide-activated surfaces **5** (—) and antibodies modified surfaces **7** prepared according to route 1 (—) and 2 (---). Since XPS analyses were done in the same conditions, the intensities are directly comparable.

Conclusions

In summary, we have described a general method to covalently immobilize antibodies on carbon surfaces. The proposed method, based on an electrochemically assisted grafting process and on the use of a monoprotected homobifunctional linker allowed the achievement of a stable and compact layer of anchored antibodies. Moreover, a better degree of coverage of the surface was obtained, compared with a classical procedure involving a homobifunctional linker. Sensitive antibodies introduced under native conditions at physiological pH, in the last step of the immobilization process, specifically recognized antigens, as shown by fluorescence competitive assay. Further investigations to extend this protocol to other types of amine-functionalized surfaces are now in progress in our laboratory.

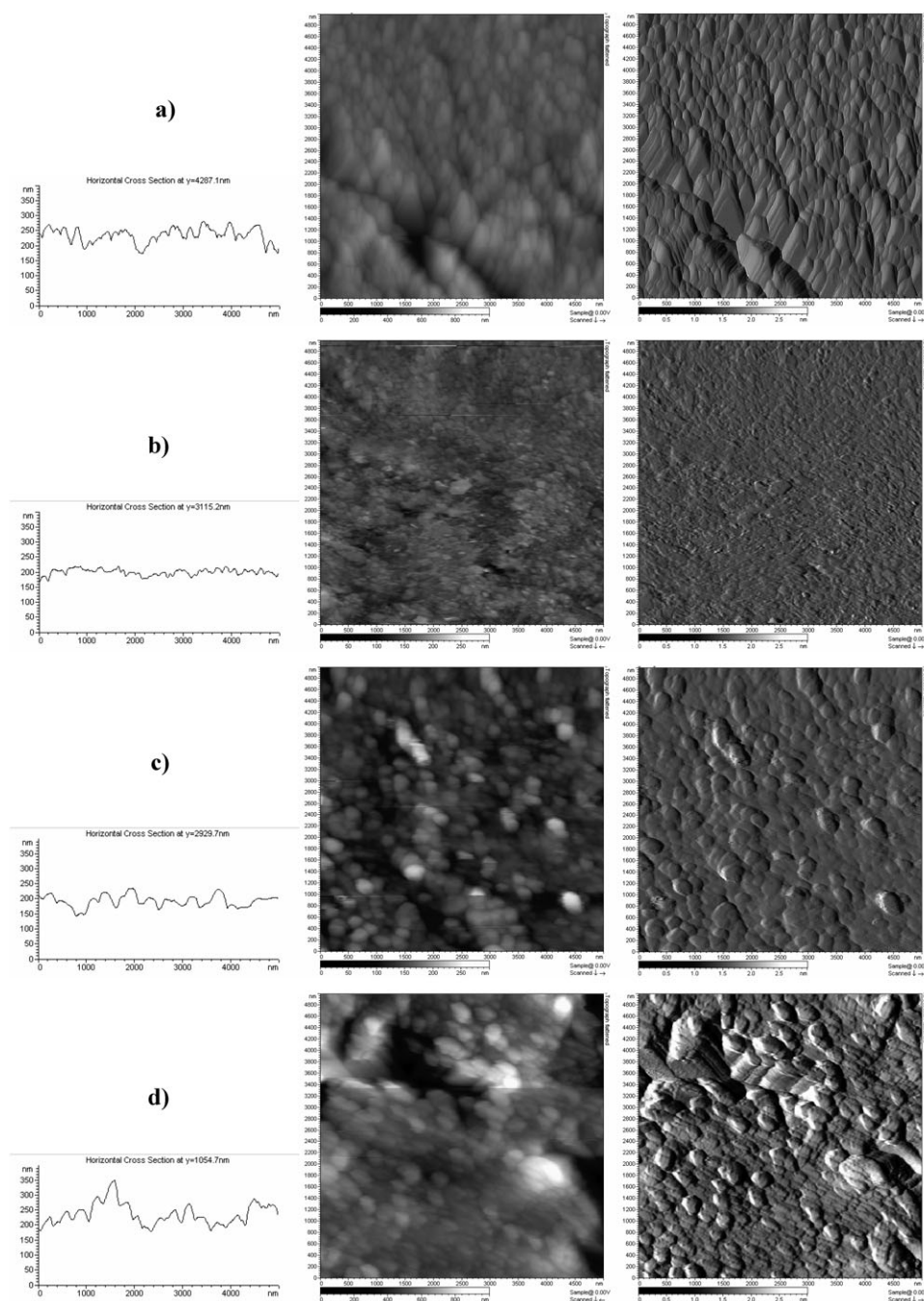


Fig. 4 Average line profiles and AFM images (left: topography and right: deflection) of polished carbon (a), *N*-hydroxysuccinimide-activated surfaces **5** (b) and antibodies modified surfaces **7** (c) after ultrasonication 3 times in PBS for 15 min (d).

Experimental

Materials

4-Nitrobenzenediazonium tetrafluoroborate, triethylamine, potassium hydroxide, 1-(3-dimethylaminopropyl)-3-ethylcarbodiimide hydrochloride, 4-nitrobenzylamine hydrochloride were purchased from Acros and methyl adipoyl chloride and *N*-hydroxysuccinimide from Aldrich. Hexanedioic acid bis-(2,5-dioxypyrrolidin-1-yl) ester was prepared according to literature.²⁶

Goat anti-human transferrin antibodies, human holo-transferrin, human serum albumin (HSA) were purchased from

Sigma and delipidated fraction V bovine serum albumin (BSA) from Roche. Texas-Red human apo-transferrin was from Molecular Probes (Eugene, OR).

Phosphate buffered saline (PBS) was prepared at pH 7.4 from 1.5 mM potassium phosphate monobasic, 8.6 mM sodium phosphate dibasic dodecahydrate, 137 mM sodium chloride, and 2.7 mM potassium chloride in deionized water.

Graphite samples, obtained by cutting a graphite rod of 20 mm diameter (Le Carbone Lorraine: 2020PT) in discs of around 5 mm thickness were polished using Struers papers (500, 1200 and 4000), diamant paste (Struers: 1 μ m) and then

alumina polishing suspensions (Struers: AP-D, OP-A μm). They were ultrasonicated 3 times in acetone and deionized water for 15 min before use.

Functionalization of graphite discs

Electrochemical treatments and analyses of the graphite samples were carried out in an electrochemical cell, containing a Saturated Calomel Electrode (SCE) as reference electrode and a graphite rod as counter electrode.

Derivatization of graphite discs: 5 mg of 4-nitrobenzenediazonium salts, dissolved in 5 ml of degassed H_2SO_4 0.5 M were reduced at $-0.2 \text{ V}_{\text{SCE}}$ for 5 min under nitrogen, using a graphite disc as working-electrode. Then the derivatized graphite disc was ultrasonicated 3 times in deionized water for 15 min.

The modified electrodes were analyzed by cyclic voltammetry in degassed H_2SO_4 0.5 M under nitrogen. First, electro-reduction of the nitro groups into hydroxylamines was performed by cycling the potential twice between 0 and $-500 \text{ mV}_{\text{SCE}}$ at 100 mV s^{-1} and then, the nitroso-hydroxylamine reversible system (Fig. 1) was observed by cycling the potential between 0 and $500 \text{ mV}_{\text{SCE}}$.

The hydroxylamino groups present on the electrode surface after analyses were subsequently reduced at $-1 \text{ V}_{\text{SCE}}$ for 10 min in the same medium to give amino groups. The disappearance of the NHOH/NO reversible system was checked for each sample. Six different samples were used for reproducibility measurements.

Route 1:

The modified electrode was then ultrasonicated in deionized water, dichloromethane and toluene before being placed in 20 ml of toluene containing 100 μl of methyl adipoyl chloride and 300 μl of triethylamine at 40°C for 3 h under nitrogen. After ultrasonication 3 times in toluene and then in dichloromethane for 15 min, they were allowed to react with an excess of potassium hydroxide in anhydrous methanol for 12 h under nitrogen at room temperature and then ultrasonicated 3 times in ethanol for 15 min.

Subsequent reaction with 1-(3-dimethylaminopropyl)-3-ethylcarbodiimide hydrochloride 0.4 M and *N*-hydroxysuccinimide 0.1 M in water for 1 h at room temperature, followed by ultrasonication 3 times in deionized water for 15 min gave the *N*-hydroxysuccinimide-activated graphite discs.

Route 2:

The modified electrode was then ultrasonicated in deionised water and anhydrous dimethylformamide before being placed in 20 ml of anhydrous dimethylformamide containing 50 mg of hexanedioic acid bis-(2,5-dioxopyrrolidin-1-yl) ester and 300 μl of triethylamine at room temperature for 5 h under argon. Then the sample was ultrasonicated twice in dimethylformamide and then in deionised water for 15 min.

These surfaces were allowed to react either with 4-nitrobenzylamine hydrochloride used as redox probe (5 g L^{-1}), either with anti-transferrin antibody (2 g L^{-1}) in pH 7.4 PBS for 3 h at room temperature. The modified graphite discs containing the redox probes were successively ultrasonicated 3 times in NaOH 0.1 M, dichloromethane, water, ethanol, acetone, acetonitrile for 15 min, before being analyzed by cyclic vol-

tammetry (reproducibility based on 5 different samples). Surfaces with covalently anchored antibodies were washed using 3 ultrasonic baths of 20 ml of pH 7.4 PBS for 10 min each, before XPS analyses.

Surface analyses

XPS analyses were performed under a base pressure of 10^{-9} mbar using a VSW HA100 spectrometer. The analyser was operated with constant pass energy of 22 eV. X-ray source used Mg K α excitation radiation at 1283.6 eV. The spectrometer binding energy scale was initially calibrated against the Au 4f (84.0 eV) level. C1s level (284.4 eV) on clean graphite disc served as a reference for all spectra. Simulation of the experimental peaks was carried out using a Gaussian-Lorentzian mixed function after background subtraction.

Topographic images were acquired in constant force mode using silicon nitride tips with an estimated radius of 10 nm on integral cantilevers. The spring constant was 0.06 N m^{-1} . The pixel size was 512×512 . Deflection signal was determined by the first derivative of the topographic signal. We used AFM Pico-plus (Molecular Imaging, Phoenix, US). The surfaces were imaged in PBS with a scan rate of 1 Hz.

Preparation of samples for fluorescent analyses were done as followed. Graphite surfaces modified with anti-transferrin antibodies (see above) were saturated by a solution of BSA (10 g L^{-1}) in PBS for 1 h at room temperature to avoid non-specific binding of antigens. Then, they were placed in a BSA solution containing $5 \mu\text{g mL}^{-1}$ of Texas Red apo-transferrin and supplemented or not with HSA ($500 \mu\text{g mL}^{-1}$) or non-labelled human apo-transferrin ($500 \mu\text{g mL}^{-1}$). After three washes in PBS, fluorescence intensity was detected using an Olympus BX microscope. The wavelengths were set at $560 \pm 20 \text{ nm}$ (excitation) and $630 \pm 37.5 \text{ nm}$ (emission). A 20×0.7 objective and acquisition times of 8s were used. Quantification of fluorescence intensity was performed from at least 4 fields of each sample by imaging analysis using SimplePCI software (Compix Inc).

Acknowledgements

This work was supported by the Agence Nationale de la Recherche (Project DEPIST), the Institut National de la Santé et de la Recherche Médicale and the Centre National de la Recherche Scientifique. We thanks Dominique Paris for carbon surface preparation, Dr Remy Le Guevel from the Cell biochips platform, Ouest Genopole and J. F. Bergamini for assistance in AFM measurements.

References

1. I. Willner and E. Katz, *Angew. Chem., Int. Ed.*, 2000, **39**, 1181.
2. Z. Dai, F. Yan, H. Yu, X. Hu and H. Ju, *J. Immunol. Methods*, 2004, **287**, 13.
3. E. Lojou and P. Bianco, *Electrochim. Acta*, 2002, **47**, 4069.
4. D. C. Alsmeyer and R. L. McCreery, *Anal. Chem.*, 1992, **64**, 1528.
5. F. Geneste, M. Cadoret, C. Moinet and G. Jezequel, *New J. Chem.*, 2002, **26**, 1261.
6. A. J. Downard, *Electroanalysis*, 2000, **12**, 1085.
7. J. Pinson and F. Podvorica, *Chem. Soc. Rev.*, 2005, **34**, 429.
8. F. Geneste and C. Moinet, *New J. Chem.*, 2005, **29**, 269.

9. P. Allongue, M. Delamar, B. Desbat, O. Fagebaume, R. Hitmi, J. Pinson and J.-M. Saveant, *J. Am. Chem. Soc.*, 1997, **119**, 201.
10. B. P. Corgier, A. Laurent, P. Perriat, L. J. Blum and C. A. Marquette, *Angew. Chem., Int. Ed.*, 2007, **46**, 1.
11. B. P. Corgier, C. A. Marquette and L. J. Blum, *Biosens. Bioelectron.*, 2007, **22**, 1522.
12. B. P. Corgier, C. A. Marquette and L. J. Blum, *J. Am. Chem. Soc.*, 2005, **127**, 18328.
13. S. E. Baker, K.-Y. Tse, C.-S. Lee and R. J. Hamers, *Diamond Relat. Mater.*, 2006, **15**, 433.
14. W. Yang, S. E. Baker, J. E. Butler, C.-S. Lee, J. N. Russell, Jr, L. Shang, B. Sun and R. J. Hamers, *Chem. Mater.*, 2005, **17**, 938.
15. S. E. Baker, K.-Y. Tse, E. Hindin, B. M. Nichols, T. L. Clare and R. J. Hamers, *Chem. Mater.*, 2005, **17**, 4971.
16. R. Blankespoor, B. Limoges, B. Schoellhorn, J.-L. Syssa-Magale and D. Yazidi, *Langmuir*, 2005, **21**, 3362.
17. G. Liu and J. J. Gooding, *Langmuir*, 2006, **22**, 7421.
18. C. Bourdillon, M. Delamar, C. Demaille, R. Hitmi, J. Moiroux and J. Pinson, *J. Electroanal. Chem.*, 1992, **336**, 113.
19. J. C. Harper, R. Polsky, D. R. Wheeler, S. M. Dirk and S. M. Brozik, *Langmuir*, 2007, **23**, 8285.
20. M. Delamar, G. Desarmot, O. Fagebaume, R. Hitmi, J. Pinson and J. M. Saveant, *Carbon*, 1997, **35**, 801.
21. T. Cao, A. Wang, X. Liang, H. Tang, W. Auner Gregory, O. Salley Steven and K. Y. S. Ng, *Biotechnol. Bioeng.*, 2007, **98**, 1109.
22. B. C. Weimer, M. K. Walsh and X. Wang, *J. Biochem. Biophys. Methods*, 2000, **45**, 211.
23. B. Xia, S.-J. Xiao, D.-J. Guo, J. Wang, J. Chao, H.-B. Liu, J. Pei, Y.-Q. Chen, Y.-C. Tang and J.-N. Liu, *J. Mater. Chem.*, 2006, **16**, 570.
24. S. S. C. Yu, E. S. Q. Tan, R. T. Jane and A. J. Downard, *Langmuir*, 2007, **23**, 11074.
25. Q. Y. Chen and G. M. Swain, *Langmuir*, 1998, **14**, 7017.
26. S. Kalkhof, C. Ihling, K. Mechtler and A. Sinz, *Anal. Chem.*, 2005, **77**, 495.